KRZYSZTOF KUBAS [*]

A TWO-DIMENSIONAL DISCRETE MODEL FOR DYNAMIC ANALYSIS OF BELT TRANSMISSION WITH DRY FRICTION

The paper presents a model for dynamic analysis of belt transmission. A two-dimensional discrete model was assumed of a belt consisting of rigid bodies joined by translational and torsion spring-damping elements. In the model, both a contact model and a dry friction model including creep were taken into consideration for belt-pulley interaction. A model with stiffness and damping between the contacting surfaces was used to describe the contact phenomenon, whereas a simplified model of friction was assumed. Motion of the transmission is triggered under the influence of torque loads applied on the pulleys. Equations of motion of separate elements of the belt and pulleys were solved numerically by using adaptive stepsize integration methods. Calculation results are presented of the reaction forces acting on the belt as well as contact and friction forces between the belt body and pulley in the sample of the belt transmission. These were obtained under the influence of the assumed drive and resistance torques.

1. Introduction

Considerations regarding friction phenomena occurring in the belt transmission go back to the eighteenth century and were initiated by Leonard Euler [1]. Euler analysed frictional forces between a belt wrapped around a fixed pulley or capstan. More important tests conducted over the centuries with specification of more important works are presented in Fawcett's work [2].

It is worth mentioning an approach used for discretisation of flexible links based on the Rigid Finite Element Method (RFEM) described in [3, 4]. The method has been successfully applied with some modifications in [5, 6]. The authors of these publications were using Lagrange equations to

---

[*] *Department of Mechanics, Faculty of Mechanical Engineering and Computer Science, University of Bielsko-Biała, ul. Willowa 2, 43-309 Bielsko-Biała, Poland; E-mail: kkubas@ath.bielsko.pl*

derive equations of motion. The stiffness and damping properties were concentrated in the dimensionless and massless spring-damping elements (SDE) and written into the equations of motion in the form of elastic strain energy and the dissipation function. In the proposed model, the same discretisation method was applied as in the classical approach of RFEM. However, in this paper Newton equations were used to derive the equations of motion. The stiffness and damping properties of the belt were included by forces written into the right side of these equations.

Works [7, 8, 9] presenting models of discrete belts are especially important from the point of view of assumptions used in the model presented in this work.

Due to the complexity of phenomena occurring in belt transmissions, it seems particularly difficult to describe friction and contact by an appropriate mathematical apparatus. The authors of [8, 10] presented a piecewise linear friction model with the possibility of predicting belt creep. It has been called the Coulomb-like tri-linear creep-rate-dependent friction model. Another sample model was presented in [11], which has been called the elastic/perfectly-plastic friction law (EPP). Normal reaction forces between the belt and pulley, which are necessary to calculate these frictional forces, can be determined using the spring-damping contact model (also known as a penalty contact model). It is often used in belt transmission models (e.g. in papers [8, 12, 13]). It was also used in this work.

The model presented below was verified by a comparison of calculation results presented in paper [12]. It was proved that, although it has a simpler mathematical apparatus, model verification was in good agreement – this is the main application aspect of this article. The model [12] was created using an "absolute nodal coordinate formulation" with a detailed contact formulation between the belt and pulley. The belt-pulley contact was formulated as a "linear complementarity problem" using the discontinuous Coulomb friction law to model frictional forces.

The next paragraph presents a mathematical apparatus of the proposed model of belt transmission. The results of verification are shown in the third paragraph. The fourth paragraph presents additional calculation results of forces acting on the belt, as well as contact and friction forces between the belt body and the pulley in another sample of the belt transmission.

2. Mathematical model

It was assumed that the belt will be treated as a system of rigid bodies connected by spring-damping elements. Since there is large bending deformation of the belt, e.g. from the curvatures of the pulleys, the tensing rollers,

it was assumed that the belt must be discretised by many bodies. This obviously influences the speed of calculations, which in turn extends the time of analyses being made. This was the reason for making some assumptions at the beginning of model development:

- the two-dimensional belt transmission model was taken into account; therefore the following phenomena were omitted: torsion rotation of the belt and influence of local changes in the cross section caused by wedging of the belt into the groove of the pulley – thus the number of degrees of freedom and the number of generalised coordinates were reduced,
- equations of motion were simplified by resigning from matrix notation in the final version, which allowed us to further reduce the number of operations performed by the computer, for example, on account of the occurrence of sparse matrices,
- it was assumed that the pulley was perfectly circular (a change in distance from the belt to the pulley centre resulted only from the kinematics of contact),
- a linear model of contact and a simplified friction model of the belt-pulley were assumed; these parameters are constant throughout the length of the belt,
- to minimise errors of numerical integration of equations of motion and to speed up the calculations it was assumed that the differential equations of motion would be solved by an adaptive stepsize method of integration – the Runge-Kutta-Fehlberg method.

The beneficial effects on the efficiency of the mathematical model were described by Schindler in [14].

Undoubtedly, discretisation of the belt brings many benefits, e.g. the ability to identify changes in the friction forces around the pulley or the distribution of axial forces along the entire length of the belt.

According to assumptions from RFEM [3, 4], it was assumed that the belt would be divided into n_b bodies. Each neighbouring pair of bodies was joined by the SDE with proper translational and bending stiffness and damping parameters (Fig. 1).

As was mentioned above, a two-dimensional model of the belt transmission was assumed. For each body i (where $i = 1 \ldots n_b$) it was assumed that there were three generalised coordinates (Fig. 2): translations x_i and y_i of the mass centre along $\mathbf{x}$ and $\mathbf{y}$ axes of the global coordinate system and body rotation with angle φ_i relative to the mass centre. Coordinate z_i always equals zero. As shown in Fig. 2, the position of the mass centre of belt body i is specified by vector $\mathbf{P}_i$.

It was also assumed that there are n_p pulleys in the transmission "lying" in the $\mathbf{xy}$ plane and rotating around the axis parallel to $\mathbf{z}$ with rotation angle
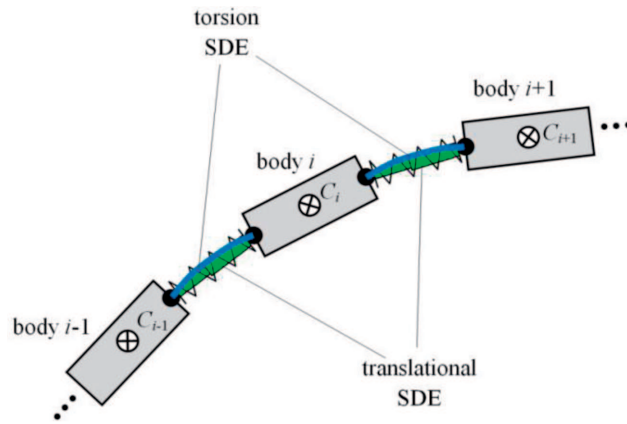
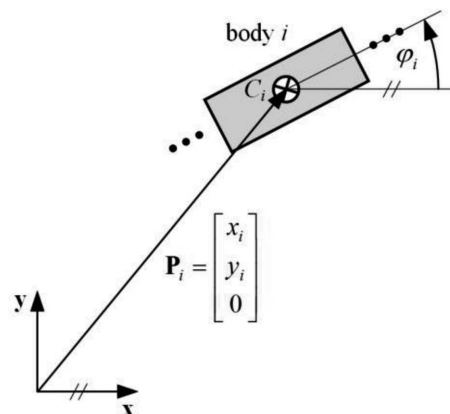Fig. 1. Assumed belt model with translational and torsion SDEs

Fig. 2. Generalised coordinates describing the position and orientation of belt body i

θ_j (where $j = 1 \ldots n_p$). Therefore, the vector of the generalised coordinates takes the form:

$$\mathbf{q}^T = \begin{bmatrix} \mathbf{q}_b^T & \mathbf{q}_p^T \end{bmatrix} = \begin{bmatrix} x_1 \ y_1 \ \varphi_1 \ \ldots \ x_i \ y_i \ \varphi_i \ \ldots \ x_{n_b} \ y_{n_b} \ \varphi_{n_b} \quad \theta_1 \ \ldots \ \theta_j \ \ldots \ \theta_{n_p} \end{bmatrix},$$
(1)

where:

$\mathbf{q}_b$ – vector of generalised coordinates of all belt bodies,

$\mathbf{q}_p$ – vector of generalised coordinates of all pulleys.

As follows from the assumptions, the number of generalised coordinates will equal $3n_b + n_p$.

First the belt was divided into n_b bodies. It was assumed that the bodies would be modelled as homogeneous thin links with mass m_i (the thickness of the segments is omitted and the centres of the masses are located in their geometric centres). The mass moment of inertia with respect to axis $\mathbf{z}_i$

perpendicular to the plane of motion and passing through the mass centre of body i equals:

$$I_{z_i} = \frac{1}{12} m_i l_i^2,$$ (2)

while the total mass of the belt equals:

$$m_b = \sum_{i=1}^{n_b} m_i.$$ (3)

Considering the specific case of the transmission, it would be advisable to check whether it is possible to assume a uniform mass distribution along the entire length of the belt. In this case, determining the mass parameters for individual bodies from equations (2) and (3) would be much simplified.

2.1. Model of the belt-pulley contact

To consider contact between the belt bodies and pulleys in the transmission, vector notation of forces was used. A diagram of the assumed distribution of forces acting on belt body i at the period of contact with pulley j is presented in Fig. 3.
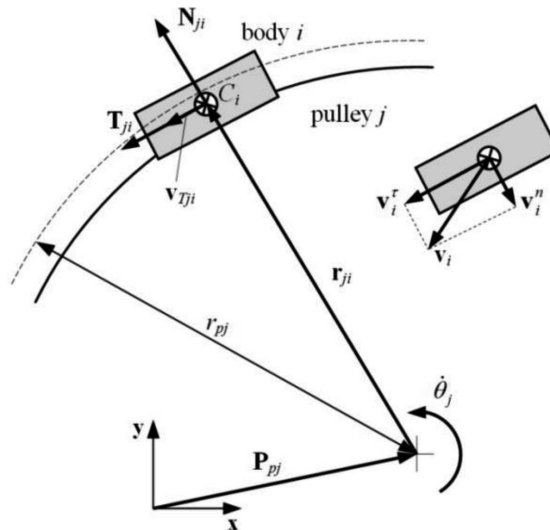

Fig. 3. Assumed configuration of velocity components of belt body i and forces acting on this body from pulley j

It was assumed that the force components, i.e. normal force $\mathbf{N}_{ji}$ and friction force $\mathbf{T}_{ji}$, would be applied to the mass centre of each body which had contact with one of the pulleys. This assumption is acceptable if the

thickness of the belt is omitted (which makes that, e.g. the distribution of stress in the cross section will not be analysed and the force of friction can be reduced to the centre C_i) and a sufficiently large number of bodies is taken to discretise the belt, so their lengths are appropriately small. It is also worth mentioning that the assumptions made are consistent with current trends in the construction of belts. These are aimed at reducing thickness in order to reduce the lateral deformation of the belt, therefore, to increase the lateral stiffness [15].

As is shown in Fig. 3, vector $\mathbf{r}_{ji}$ is orientated from the centre of pulley j to the mass centre of body i. If there is contact between the body and the pulley, but the value of normal force $\mathbf{N}_{ji}$ is still zero, the length of this vector equals an arbitrary value r_{pj}. Thus, at the time of non-zero normal force (the situation shown in the figure) there is an inequality: $r_{ji} < r_{pj}$. The position of the pulley centre in the global coordinate system is specified via vector $\mathbf{P}_{pj}$.

Vector $\mathbf{r}_{ji}$ can be determined from the following formula:

$$\mathbf{r}_{ji} = \mathbf{P}_i - \mathbf{P}_{pj}. \tag{4}$$

A versor (unit vector) according to the direction and sense of vector $\mathbf{r}_{ji}$ equals:

$$\hat{\mathbf{r}}_{ji} = \frac{\mathbf{r}_{ji}}{\left|\mathbf{r}_{ji}\right|}. \tag{5}$$

Penetration depth of belt body i with pulley j can be determined from the formula:

$$p_{ji} = r_{pj} - \left|\mathbf{r}_{ji}\right|. \tag{6}$$

Assuming that the linear velocity of the centre of the pulley is zero, the value of penetration velocity $\dot{p}_{ji}$ is equal to the value of the normal velocity component $\mathbf{v}_i^n$ (Fig. 3). This value was determined on the basis of the following scalar product:

$$\dot{p}_{ji} = \left|\mathbf{v}_i^n\right| = -\mathbf{v}_i^T \cdot \hat{\mathbf{r}}_{ji}, \tag{7}$$

where:

$\mathbf{v}_i$ − velocity of the mass centre of body i.

Since the contact force $\mathbf{N}_{ji}$ formed during contact between body i and pulley j has a consistent direction with the direction of the radius versor $\hat{\mathbf{r}}_{ji}$, then:

$$\mathbf{N}_{ji} = N_{ji}\hat{\mathbf{r}}_{ji}. \tag{8}$$

The value of this force was determined in a similar form as given in paper [16], in which the authors proved a nonlinear relation between the penetration depth and the normal force:

$$N_{ji}\left(p_{ji}, \dot{p}_{ji}\right) = c_1 p_{ji}^2 + c_2 p_{ji} + \delta\left(p_{ji}\right) b \dot{p}_{ji}, \tag{9}$$

where:

c_1, c_2 – belt-pulley contact stiffness coefficients,
b – belt-pulley contact damping coefficients.

Figure 4 shows graphically the course of function $\delta(p_{ji})$ used in equation (9).
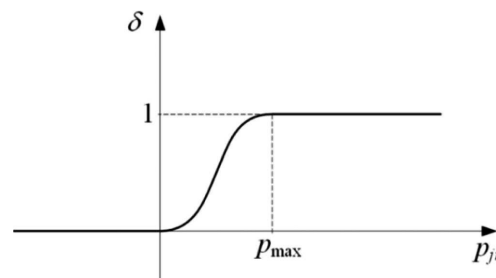

Fig. 4. A course of function $\delta(p_{ji})$

In this model it is assumed that for $p_{ji} \leq 0$, force $\mathbf{N}_{ji}$ will be zero. At the period of contact, for p_{ji} not much greater than zero, only stiffness has an influence. The application of function $\delta(p_{ji})$ results in the fact that in the range of $0 < p_{ji} < p_{max}$ the influence of the damping force component is increased (from 0 to $b\dot{p}_{ji}$). It achieves "full damping" (component $b\dot{p}_{ji}$ is then fully taken into the formula) beyond a certain arbitrary value of p_{max}. This procedure makes it possible to avoid such an effect of "sticking up" elements at the initial period of contact (in particular when velocity $\dot{p}_{ji}$ is relatively high).

To ensure a smooth shape of the transition function $\delta(p_{ji})$ from zero damping to "full damping" (as shown in Fig. 4), it was described by the function of the state consisting of constant functions and a third-degree polynomial in certain ranges, which can be defined by the following generalised formula:

$$y(x) = \begin{cases} y_0, & \text{for } x \leq x_0, \\ y_0 + (y_1 - y_0)\, d^2\,(3 - 2d), & \text{for } x_0 < x < x_1, \\ y_1, & \text{for } x \geq x_1, \end{cases} \qquad (10)$$

where:

$$d = \frac{x - x_0}{x_1 - x_0}.$$

The function above is continuous and satisfies the condition of continuity of the first derivative at points x_0 and x_1. After replacing the values: $x_0 = 0$,

$y_0 = 0$, $x_1 = p_{\max}$ and $y_1 = 1$, function $\delta(p_{ji})$ was obtained in the following form:

$$\delta\left(p_{ji}\right) = \begin{cases} 0, & \text{for } p_{ji} \leq 0, \\ \left(\dfrac{p_{ji}}{p_{\max}}\right)^2 \left(3 - 2\dfrac{p_{ji}}{p_{\max}}\right), & \text{for } 0 < p_{ji} < p_{\max}, \\ 1, & \text{for } p_{ji} \geq p_{\max}. \end{cases} \tag{11}$$

The use of equations (9)-(11) enabled us to make the damping force component as a function of both penetration velocity $\dot{p}_{ji}$ and penetration depth p_{ji} in contact. It should also be noted that these relations are widely used in contact models. A similar model was used by the MSC.Adams software [17].

2.2. Friction model

A simplified model including the velocity-dependent curve of the friction coefficient was used to determine friction forces. In this model, the classic approach to the phase of static friction, whose modelling is difficult because of the change in number of solved equations, was neglected. The friction force is unknown if two moving bodies stick, therefore an additional constraint equation must be included. The friction force is known for their relative motion, so we need to determine only differential equations of motion. It is worth mentioning that during integration of differential equations of motion it is difficult to identify moments of changes in the state of friction. The static friction phase can be omitted due to the friction coefficient dependence on the value of relative velocity v in contact. The formula by which the value of friction force $\mathbf{T}$ is determined in this case takes the following form:

$$T = \mu(v) N. \tag{12}$$

Figure 5 shows a simplified form of the friction coefficient curve assumed by Threlfall [18]. As can be seen, value Δv is an arbitrary value of velocity v from which the kinetic friction coefficient μ_k is taken.

The curve shown above can be used by assuming only the kinetic friction coefficient μ_k. As is shown in [16], in the case of cooperating surfaces of the belt and pulley, these coefficients may differ from each other. This fact should be included in the assumed curve of the friction coefficient.

The assumptions used here are incompatible with those of Coulomb friction law, where it is assumed that static friction occurs only at zero velocity. As it turns out, in fact, creep can occur in the state of sticking of two surfaces (at the instance of static friction). This phenomenon was first investigated in-depth in 1926 independently by Wierchowsky and Rankin [19], and has been the subject of many works, such as the already classic
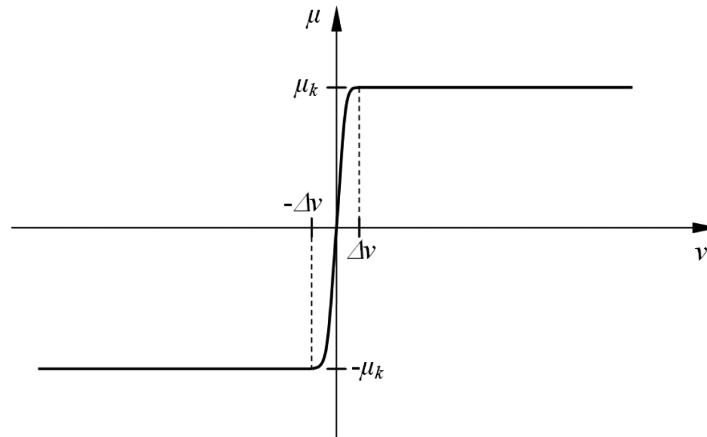
Fig. 5. Simplified form of the friction coefficient curve [18]

publication by Bowden and Tabor [20], or the widely cited Dahl paper [21]. The oldest paper which is known to the author of this paper and which shows the results of an investigation into the existence of the creep phenomenon in belt transmissions is a paper written in 1847 by Reynolds [22].

In the analysed case, for such an elastic contact, which is the contact between surfaces of rubber and steel, it should be assumed that the creep phenomenon occurs in the velocity range to Δv. In a majority of cases (except for the case of the toothed belt) such a slip occurs (including creep) in the transmission between the belt and the pulley, although it is different for different types of belts. An evaluation of the intensity of this phenomenon for a specific type of belt transmission could be made after performing relevant experimental studies, which may be conducted in the future by the author. How different velocity-dependent friction curves for different types of belts can be is shown by examples of different assumptions of friction models (assuming them as functions of different variables, a different degree of non-linearity) presented in papers [8, 9, 16]. Some of them are determined empirically.

Thus, in order to present the phenomena occurring in the velocity $v < \Delta v$ more accurately we decided to make the friction coefficient a function of creep (therefore, also of the creep velocity).

As can be seen in Fig. 3, the tangential component of the relative velocity between pulley j and belt i was marked $\mathbf{v}_{Tji}$. The functional dependence of the coefficient of friction in the velocity values $v_{Tji} < \Delta v$ was determined using the formula:

$$\mu\left(\Delta_{Tji}, v_{Tji}\right) = (1 - \beta)\mu_1 + \beta\mu_s, \tag{13}$$

where:

Δ_{Tji} – creep value (calculated as product of velocity and elementary time: $\Delta_{Tji} = v_{Tji}\Delta t$).

The coefficients β and μ_1 present in equation (13) were defined as the functions of transition velocity Δv (in the case of coefficient β) and the maximum of creep $\Delta_{\max}$ (in the case of coefficient μ_1) as the courses shown in Fig. 6a and b.
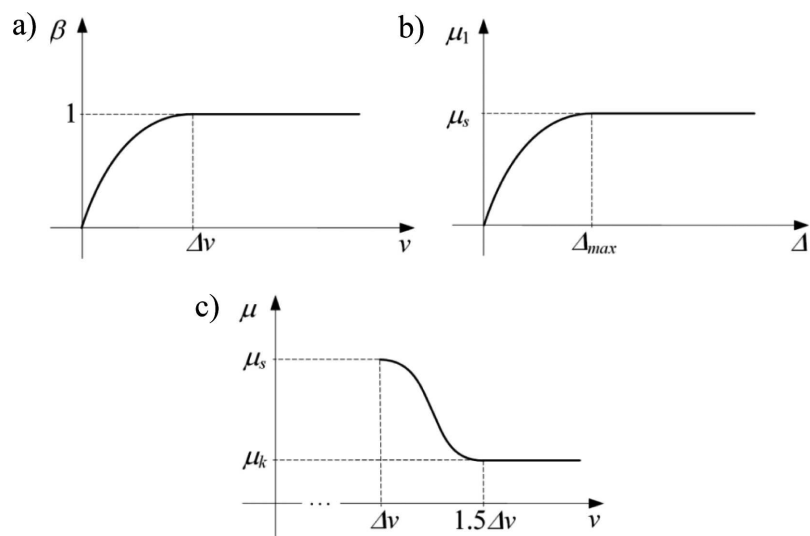

Fig. 6. Courses of coefficients: a) $\beta(v)$, b) $\mu_1(\Delta)$, c) $\mu(v)$

Figure 6c shows a change in the friction coefficient in velocity values $v_{Tji} > \Delta v$. As can be seen in the velocity values $\Delta v < v_{Tji} < 1.5\Delta v$, the value of coefficient μ changes "smoothly" from μ_s to μ_k. Above a velocity value of $1.5\Delta v$ the value μ is constant: $\mu = \mu_k$. The courses shown in Fig. 6 were made using a similar function, which is presented in Fig. 4 and which is presented in the form of a generalised formula (10). The courses shown in Fig. 6a and b were interpreted as half of this course.

It should be noted that a similar method of determining friction forces in joints to the one presented here was proposed in MSC.Adams software [17].

To determine the friction coefficient it was necessary to calculate the linear velocity vector of the contact point of pulley j with belt body i:

$$\mathbf{v}_{pj} = \dot{\theta}_j \times \hat{\mathbf{r}}_{ji}, \tag{14}$$

where:

$$\dot{\theta}_j = \begin{bmatrix} 0 \\ 0 \\ \dot{\theta}_j \end{bmatrix} - \text{vector of the angular velocity of pulley } j.$$

Considering the case of friction of belt body i with pulley j, one must determine the tangential component of the velocity vector of the mass centre of body i:

$$\mathbf{v}_i^\tau = \left(\mathbf{v}_i^T \hat{\boldsymbol{\tau}}_{ji} \right) \hat{\boldsymbol{\tau}}_{ji}. \tag{15}$$

In the above formula, versor $\hat{\boldsymbol{\tau}}_{ji}$ parallel to the tangent passing through the mass centre of body i must be known and can be determined by using the following formula:

$$\hat{\boldsymbol{\tau}}_{ji} = \frac{\boldsymbol{\tau}_{ji}}{\left| \boldsymbol{\tau}_{ji} \right|} = \frac{\hat{\mathbf{Z}} \times \hat{\mathbf{r}}_{ji}}{\left| \boldsymbol{\tau}_{ji} \right|}. \tag{16}$$

Since the angle between versors $\hat{\mathbf{Z}}$ and $\hat{\mathbf{r}}_{ji}$ is constant and always equals $90°$ (because, as was already mentioned, the pulley "lies" in the **xy** plane and the axis of rotation is parallel to the **z** axis), so $\left| \hat{\mathbf{Z}} \times \hat{\mathbf{r}}_{ji} \right| = 1$, then the formula (16) can be simplified:

$$\hat{\boldsymbol{\tau}}_{ji} = \hat{\mathbf{Z}} \times \hat{\mathbf{r}}_{ji}. \tag{17}$$

In practice, during a pulley rotation versor $\hat{\boldsymbol{\tau}}_{ji}$ has a direction and sense consistent with the direction and positive sense of velocity vector $\mathbf{v}_{pj}$. However, in the absence of a rotation of pulley j (when $\mathbf{v}_{pj} = 0$) the tangential direction to the pulley can be identified by $\hat{\boldsymbol{\tau}}_{ji}$ (determining the versor from zero vector $\mathbf{v}_{pj}$ is impossible in this case).

Therefore, the relative velocity between both moving elements is:

$$\mathbf{v}_{Tji} = \mathbf{v}_{pj} - \mathbf{v}_i^\tau. \tag{18}$$

The friction force was defined as:

$$\mathbf{T}_{ji} = \boldsymbol{\mu} \left(\Delta_{Tji}, \mathbf{v}_{Tji} \right) N_{ji}, \tag{19}$$

where:

$\boldsymbol{\mu} \left(\Delta_{Tji}, \mathbf{v}_{Tji} \right) = \mu \left(\Delta_{Tji}, v_{Tji} \right) \hat{\mathbf{v}}_{Tji}$ − vector notation of the friction coefficient,

$\hat{\mathbf{v}}_{Tji}$ − versor consistent with the direction and sense of $\mathbf{v}_{Tji}$.

As can be seen, the above equation has a modified form of equation (12).

It should be noted that the belt transmission model developed here can take into account the presence of tensing rollers. In this case, other contact and friction parameters at the belt-roll contact should be considered.

Moreover, the assumed friction model does not include separate sticking and sliding zones on the circumference of the pulley. The author is aware of the fact that, if these zones were included, a more accurate representation of phenomena occurring between the pulley and belt could be developed. Therefore, the author plans to consider them in future work.

2.3. Equations of motion

A diagram of the assumed distribution of forces and torques acting on body i from the neighbouring bodies is shown in Fig. 7.
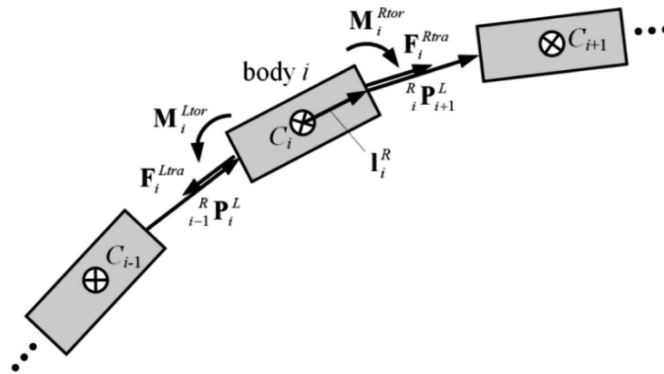

Fig. 7. Assumed configuration of forces and torques acting on belt body i from neighbouring bodies

The values of forces and torques in the translational and torsion SDEs connecting body $i-1$ with body i are described by the Kelvin-Voigt [23] relations:

$$F_i^{Ltra} = F_{i-1}^{Rtra} = c_{tra}\Delta l_i^L + b_{tra}\Delta \dot{l}_i^L, \qquad (20)$$

$$M_i^{Ltor} = M_{i-1}^{Rtor} = c_{tor}\left(\varphi_i - \varphi_{i-1}\right) + b_{tor}\left(\dot{\varphi}_i - \dot{\varphi}_{i-1}\right), \qquad (21)$$

where:

F_i^{Ltra}, F_i^{Rtra} – values of forces in translational left SDE (connecting body i with body $i-1$) and right SDE (connecting body i with body $i+1$), respectively,

M_i^{Ltor}, M_i^{Rtor} – values of bending torques in torsion left SDE and right SDE, respectively,

c_{tra}, b_{tra} – stiffness and damping coefficients in translational SDE,

c_{tor}, b_{tor} – stiffness and damping coefficients in torsion SDE,

$\Delta l_i^L = \Delta l_{i-1}^R = \left|{}_{i-1}^R\mathbf{P}_i^L\right|$ – deformation of translational SDE,

$\Delta \dot{l}_i^L = \Delta \dot{l}_{i-1}^R = v_i^{L'} - v_{i-1}^{R'}$ – velocity of deformation of translational SDE,

$v_i^{L'} = \left(\mathbf{v}_i^L\right)^T {}_{i-1}^R\hat{\mathbf{P}}_i^L$, $v_{i-1}^{R'} = \left(\mathbf{v}_{i-1}^R\right)^T {}_{i-1}^R\hat{\mathbf{P}}_i^L$ – projections of velocity vectors $\mathbf{v}_i^L$ and $\mathbf{v}_{i-1}^R$ on vector ${}_{i-1}^R\hat{\mathbf{P}}_i^L$,

${}_{i-1}^R\hat{\mathbf{P}}_i^L$ – versor consistent with the direction and sense of vector ${}_{i-1}^R\mathbf{P}_i^L$.

Vector ${}_{i-1}^R\mathbf{P}_i^L$ can be calculated using the following form:

$$_{i-1}^R\mathbf{P}_i^L = \mathbf{P}_i - \mathbf{l}'_i - \mathbf{P}_{i-1} + \mathbf{l}'_{i-1}. \qquad (22)$$

where:

$$\mathbf{l}'_i = \begin{bmatrix} \dfrac{l_i}{2}\cos\varphi_i \\[2mm] \dfrac{l_i}{2}\sin\varphi_i \\[2mm] 0 \end{bmatrix} \quad - \quad$$ vector with the direction and half the length of body i (vector $\mathbf{l}'_{i-1}$ is determined in the same way).

Force $\mathbf{F}_i^{Ltra}$ has a direction consistent with the direction of vector $_{i-1}^{R}\mathbf{P}_i^L$ but has opposite sense, while force $\mathbf{F}_i^{Rtra}$ has a direction and sense consistent with the direction and sense of vector $_i^R\mathbf{P}_{i+1}^L$ (in case of zero values of lengths $_i^R\mathbf{P}_{i+1}^L$ and $_i^R\mathbf{P}_{i+1}^L$ the direction of $\mathbf{F}_i^{Ltra}$ and $\mathbf{F}_i^{Rtra}$ is taken from last time-step). As can be seen in Fig. 7, these vectors determine the direction, sense and magnitude of the longitudinal displacement of SDEs connecting bodies $i-1$ with i and i with $i+1$. Equations of motion of body i take the form:

$$\begin{cases} m_i\ddot{x}_i &= \left(\mathbf{F}_i^{Ltra} + \mathbf{F}_i^{Rtra} + \displaystyle\sum_{j=0}^{n_p-1}(\mathbf{N}_{ji} + \mathbf{T}_{ji}) + m_i\mathbf{g}\right)\hat{\mathbf{X}}^T, \\[4mm] m_i\ddot{y}_i &= \left(\mathbf{F}_i^{Ltra} + \mathbf{F}_i^{Rtra} + \displaystyle\sum_{j=0}^{n_p-1}(\mathbf{N}_{ji} + \mathbf{T}_{ji}) + m_i\mathbf{g}\right)\hat{\mathbf{Y}}^T, \\[4mm] I_{z_i}\ddot{\varphi}_i &= \left(\mathbf{M}_i^{Ltra} + \mathbf{M}_i^{Rtra} + \mathbf{M}_i^{Ltor} + \mathbf{M}_i^{Rtor}\right)\hat{\mathbf{Z}}^T, \end{cases} \tag{23}$$

where:

$\hat{\mathbf{X}}^T = [1\ 0\ 0]\,, \hat{\mathbf{Y}}^T = [0\ 1\ 0]\,, \hat{\mathbf{Z}}^T = [0\ 0\ 1]$ $-$ versors consistent with axes **x y z,** respectively of the global coordinate system,

$\mathbf{M}_i^{Ltra} = -\mathbf{l}'_i \times \mathbf{F}_i^{Ltra}$,

$\mathbf{M}_i^{Rtra} = \mathbf{l}'_i \times \mathbf{F}_i^{Rtra}$,

$\mathbf{g}$ – vector of gravitational acceleration.

Equations (23) were simplified in the process of developing a computer model. The corresponding components of the vectors given in parentheses on the right-hand sides were thus reduced. It was assumed that the pulleys' move will take place from the set torques. The equation of motion of pulley j will have the form:

$$I_{z_j}\ddot{\theta}_j = M_{dj} - \sum_{i=0}^{n_b-1}\mathbf{M}_{Tji}\hat{\mathbf{Z}}^T, \tag{24}$$

where:

I_{z_j} – mass moment of inertia of pulley j,
M_{dj} – value of the set torque,
$\mathbf{M}_{Tji} = \hat{\mathbf{r}}_{ji} \times \mathbf{T}_{ji}$ – friction torque acting from belt body i.

The resistance torque acting on the pulley can be included in the assumed model. A negative value of M_{dj} (e.g. constant or dependent on velocity $\dot{\theta}_j$) should be taken in this case.

3. Model verification

Parameters of the transmission model discussed in the paper were implemented into the sample transmission presented in [12]. The assumed number of bodies was 60. The parameters of the transmission were taken into account from [12]:

$$c_{tra} = 10^4 \text{ N/m}, \qquad b_{tra} = 0.5 \text{ Ns/m},$$
$$c_{tor} = 0.0208 \text{ Nm/rad}, \qquad b_{tor} = 0,$$
$$c_1 = 0, \qquad c_2 = 5 \cdot 10^6 \text{ N/m},$$
$$b = 300 \text{ Ns/m}, \qquad p_{max} = 0.001 \text{ m},$$
$$\Delta v = 10^{-5} \text{ m/s}, \qquad \Delta_{max} = 10^{-4} \text{ m},$$
$$m_i = 1.036 l_i \text{ kg}, \qquad I_{z_1} = I_{z_2} = 0.02 \text{ kgm}^2.$$

The pulleys have the same radius $r_{p1} = r_{p2} = 0.08125$ m. The distance between the pulleys is $l_p = 0.253$ m. According to [12], identical values of static and kinetic friction $\mu_s = \mu_k = 0.8$ were assumed. Additionally, the same courses of the angular velocity of the drive pulley and resistance torque acting on the driven pulley were assumed, and these are shown in Figs 8 and 9, respectively.
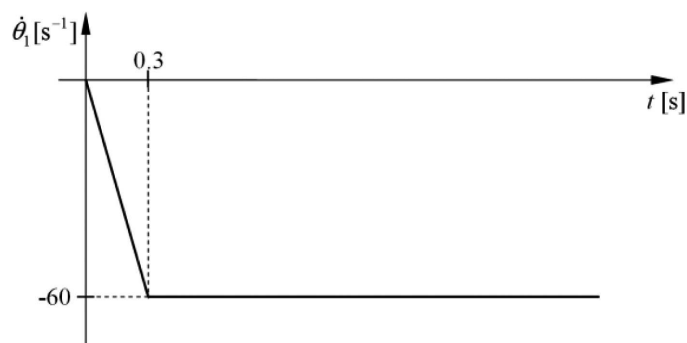

Fig. 8. Assumed course of angular velocity of the drive pulley

In this model, the course of angular velocity of the drive pulley was assumed instead of the differential equation of motion. This led to a reduction in the number of equations.

Figure 10 shows a comparison of driven pulley angular velocity courses obtained by [12] and by the model presented in this paper.
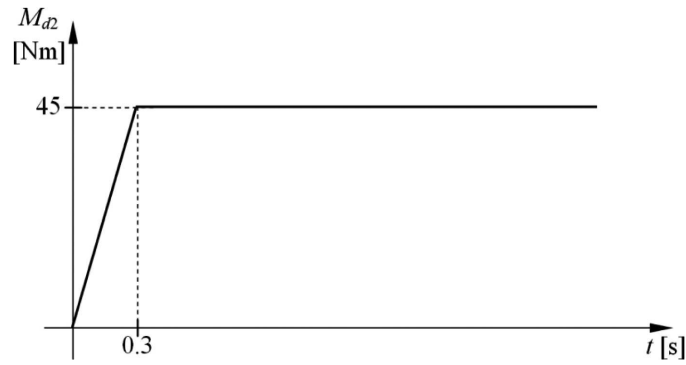
Fig. 9. Assumed course of torque acting on the driven pulley

The course presents torsional vibrations of the driven pulley under the influence of a change in the course of resistance torque at a time of 0.3s.
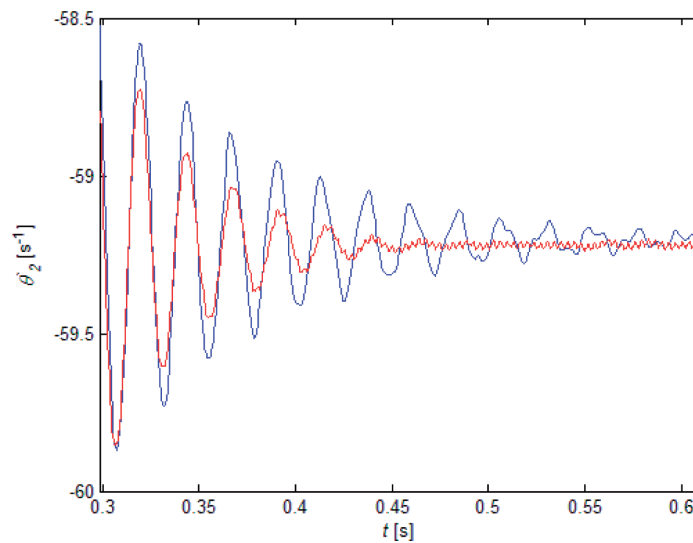

Fig. 10. Comparison of courses of angular velocity of the driven pulley — compared course [12], — calculated course

Fairly good agreement of the results, especially in the case of the value of the transmission slip and the frequency of vibration, can be seen in the presented course. At the same time, greater damping of the belt model presented in this paper was observed, and it resulted in a lower amplitude and faster reduction of vibrations presented in the graph. The reasons for these differences will be investigated in future studies.

4. Calculation results

Parameters of another sample transmission with the belt were taken on the basis of papers [12, 13, 16]:

$$c_{tra} = 1.52 \cdot 10^5 \text{ N/m}, \qquad b_{tra} = 20.5 \text{ Ns/m},$$
$$c_{tor} = 0.026 \text{ Nm/rad}, \qquad b_{tor} = 0,$$
$$c_1 = 3.0256 \cdot 10^9 \text{ N/m}^2, \qquad c_2 = 6.5 \cdot 10^5 \text{ N/m},$$
$$b = 300 \text{ Ns/m}, \qquad p_{\max} = 0.001 \text{ m},$$
$$\Delta v = 10^{-5} \text{ m/s}, \qquad \Delta_{\max} = 10^{-4} \text{ m},$$
$$m_i = 0.096 l_i \text{ kg}.$$

According to information included in [13, 16], the poly-V belt type 5pk with a length of 1.2m was analysed. These belts are used in heavily loaded transmission and work in conditions of high speeds. The above transmission parameters were adopted in accordance with data given in [13]. The analysed transmission does not have tensing rollers. The pulleys have the same radius $r_{p1} = r_{p2} = 0.027$ m. The distance between the pulleys is $l_p = 0.515$ m. Mass moments of inertia of the pulleys were taken as $I_{z_1} = I_{z_2} = 2.4 \cdot 10^{-4}$ kg m^2. Due to the relatively small radius of the pulleys, the belt had to be discretised by a sufficiently large number of bodies. The number of bodies was determined by appropriate (satisfactory) mapping of curvatures of the belt lying on the pulleys, which, as it turned out from the numerical tests, had a significant influence on the accuracy of mapping the contact phenomena and results slip. Finally, 150 bodies of equal length were taken for analysis.

The belt was tensed preliminarily in such a way that the preload force value was slightly greater than 550N. The coefficients of friction were assumed according to information contained in [16]. It was assumed that coefficients for both pulleys would be the same. The coefficient of static friction is taken as $\mu_s = 1.05$ and the coefficient of kinetic friction as $\mu_k = 1$.

The global coordinate system was taken in such a way that the **z** axis coincided with the centre of rotation of the drive pulley and the **y** axis was directed opposite to the vector of gravity (in the up direction). The **x** axis was directed to the centre of the driven pulley. The assumed parameters of belt transmission with the assumed global coordinate system are illustrated in Fig. 11.

As has already been mentioned while presenting equations of motion, drive torque $\mathbf{M}_{d1}$ as the time course acting on the drive pulley in the form shown in Fig. 12 (with the direction and sense shown in Fig. 11) was taken
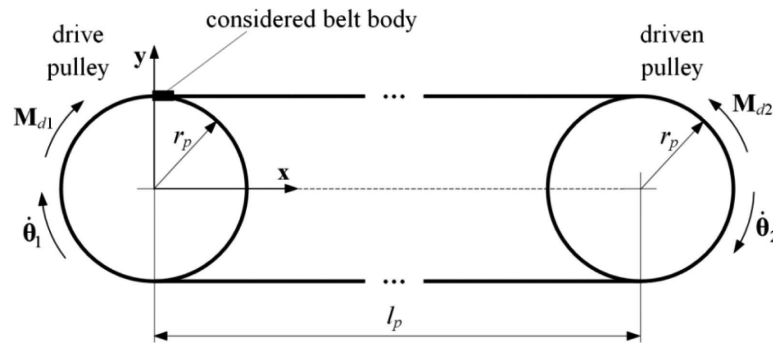
Fig. 11. Assumed parameters of the transmission analysed

for the analysis. It was assumed that at a time of 0.3 s it reaches a value of 15 Nm. After this time the value remains constant.
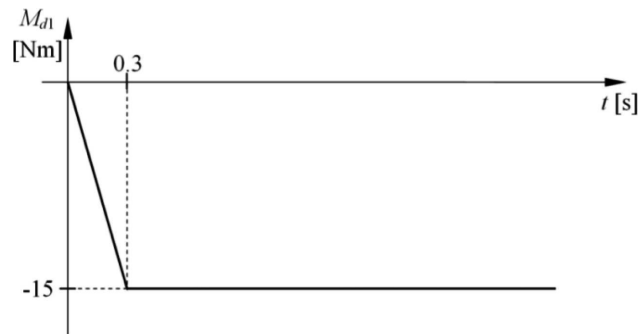

Fig. 12. Assumed course of torque acting on the drive pulley as a function of time

It was also assumed that resistance torque $\mathbf{M}_{d2}$ as a function of the angular velocity of the pulley would be applied on the driven pulley. A value of 15 Nm (which is equal to the value of the applied torque to the drive pulley) is reached at a driven pulley velocity of 4 rad/s. The course of this torque (with the direction and sense shown in Fig. 11) was shown in Fig. 13.

The assumed values of the belt preload and the drive and resistance torques should result, in the case of perfect transmission without belt creep and slip presence, in an approximately two-fold, in relation to the preload, increase in the reaction force in the active part of the belt, and should reduce this force to nearly zero in the case of the passive belt. Since there are creeps, slips and vibrations present there, this imbalance is reduced partially.

Transmission movement was obtained under the influence of the applied drive and resistance torques. Figure 14 shows the angular velocities obtained in the drive and the driven pulley. As can be seen, after a time of 0.3 s the velocity of the drive pulley (corresponding torque 15 Nm) reached a value
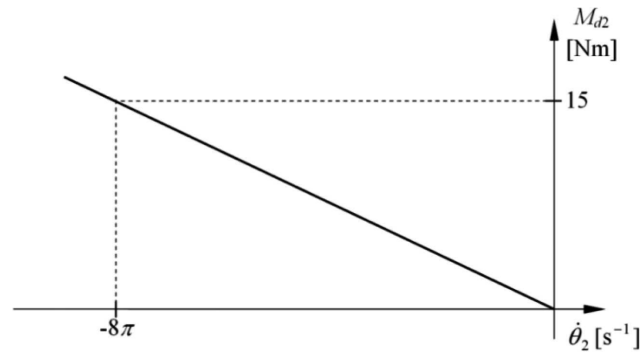
Fig. 13. Assumed course of torque acting on the driven pulley as a function of the angular velocity

of about -22.5 rad/s and no longer increased. The value angular velocity of the driven pulley is definitely lower than should be expected (reading in Fig. 13 it should be $-8\pi = -25.1$ rad/s) because of energy dissipation from the SDEs, friction and contact between the belt and the pulleys.
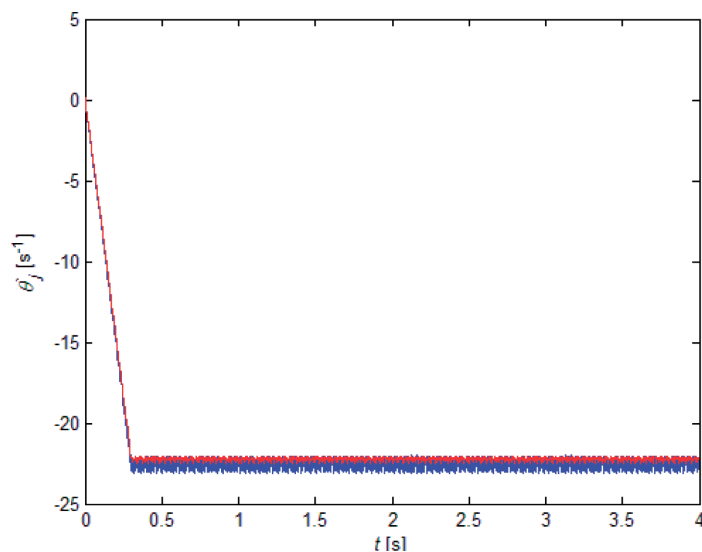

Fig. 14. Calculated courses of the angular velocities of the pulleys a) — drive pulley, b) — driven pulley

It should be mentioned that the slip was almost 1.5% after the transmission started rotating to the applied velocity. This value may depend on the resistance torque assumed and the initial belt tension, it can also depend on other assumptions of the model, including parameters of friction and contact. As was mentioned previously, this subject will be considered by the author in the future.

It was decided to look at a specific body (which is marked in Fig. 11) and a neighbouring SDE to obtain the corresponding time courses of the reaction forces from the pulley and the neighbouring bodies.

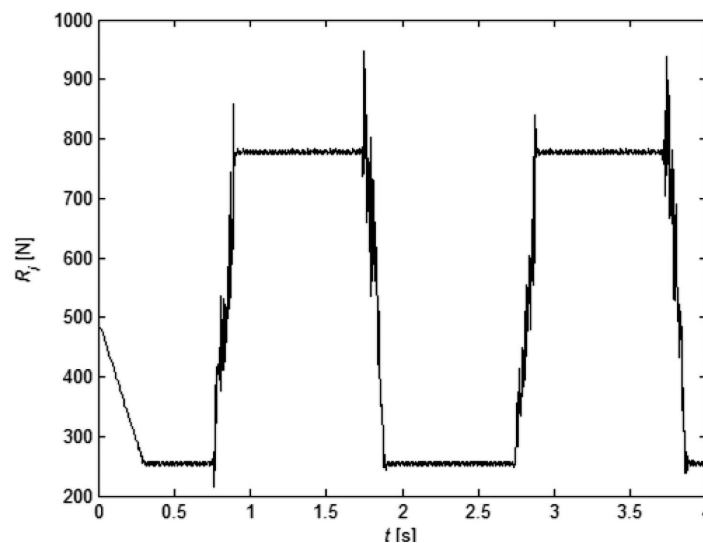Figure 15 shows the time course of the force in the selected translational SDE.

Fig. 15. Calculated course of the values of force in the selected translational SDE

In the presented course it can be seen that the force changes its values in the ranges. At the initial moment, when the transmission begins working, there is a short-term stability phase. In the analysed time interval to 0.75 s the SDE was located in the passive (top) part of the belt. In this case, after the transmission start phase the force value was about 250 N. After this time the force increased rapidly to reach a value of about 780 N in a time interval of about 0.9-1.74 s. At this time the SDE was in the active (bottom) part of the belt. It can be seen that next it passed several times to the passive and the active part of the belt. The time intervals of rapidly changing forces correspond to moments of relatively short-time interaction of the body with the pulleys.

The next courses present normal forces from the pulleys reacting on the selected body of the belt (Fig. 16) and the friction force (Fig. 17) as a result of activity of the normal force.

According to general knowledge of belt transmission, included, among others, in work [15], the normal force decreases gradually on the circumference of the drive pulley (viewed in the direction from the active to the passive part of the belt) and increases gradually on the circumference of the driven pulley (viewed in the direction from the passive to the active part
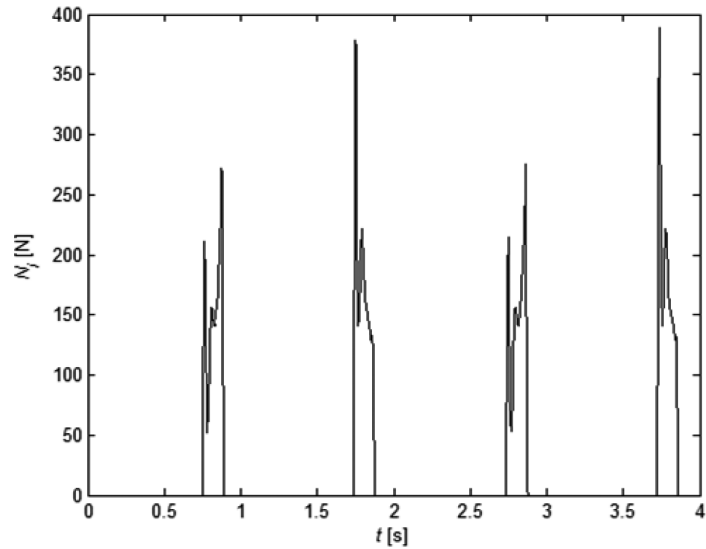
Fig. 16. Calculated course of values of the normal force acting on the selected belt body from the pulleys
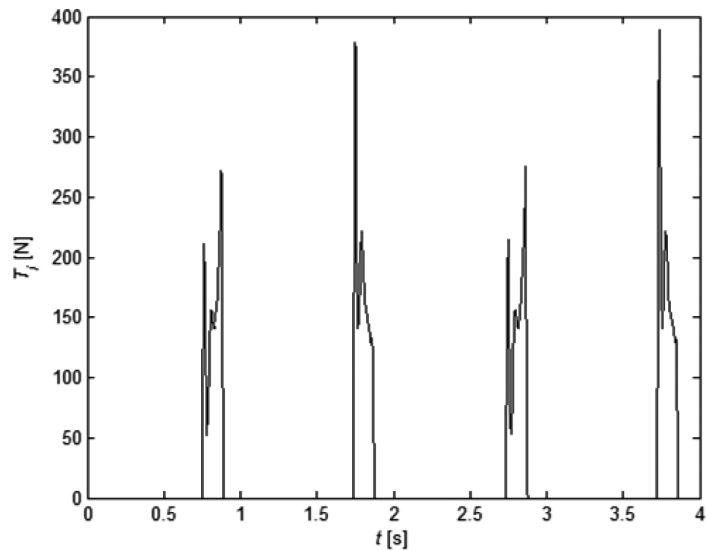

Fig. 17. Calculated course of values of the friction force between the pulleys and the selected belt body

of the belt). This relation can be seen in Fig. 16. First, the analysed belt body passes through the driven pulley (the first part of the increasing non-zero values of normal forces) and then passes through the drive pulley (the second part of nonzero decreasing values of normal forces).

Especially interesting is the fact that Fig. 16 and Fig. 17 are similar. Since the values of coefficients of static and kinetic friction taken from work [16]

are close to unity, it must be concluded that predominantly the friction force is near the fully developed value (in the case of stickiness), or that the slip is present in the contact. To check which case of friction appears, selected belt element-pulley relative velocity values v_{Tji} are shown in Fig. 18.
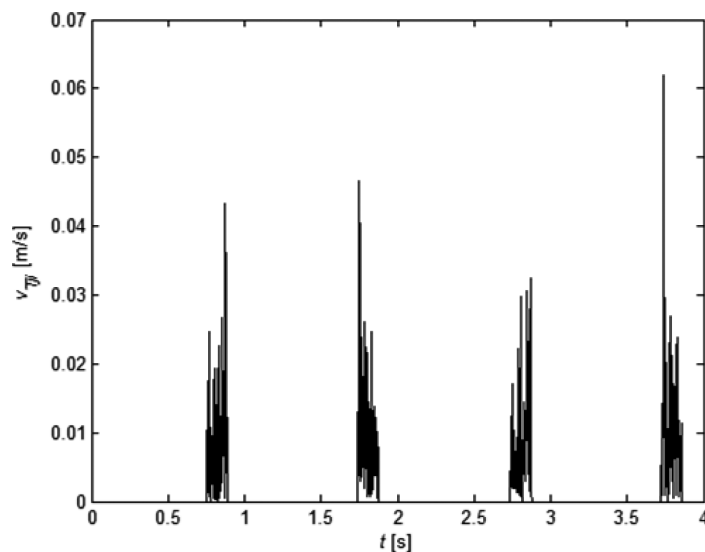

Fig. 18. Relative velocity values v_{Tji} between selected belt body and pulleys

In the cases of belt-pulley contact and assumed friction model, the values shown in Fig. 18 definitely exceed the arbitrary velocity $1.5\Delta v = 1.5 \cdot 10^{-5}$. This means that only belt slip occurs in the calculations.

5. Summary

The proposed method of dynamic analysis of belt transmission and the presented sample results do not completely cover the discussed topics but are just the beginning of considerations. Application of the friction model with creep undoubtedly offers many opportunities, but it should be emphasised that these opportunities should be supported by experimental studies. It is particularly important to identify the parameters describing the physical properties of the belt, including its stiffness and damping properties, as well as friction and contact between the belt and the pulleys or the tensing rollers. These types of studies were conducted in the cited papers [13, 16].

In the future the author will focus on the use of multithreading to determine the contact forces of individual belt bodies from the pulleys. The author of paper [14] noticed that multithreading significantly affects the speed of calculation. This is caused by better adaptation of the application that was

developed for multi-core processors which are most commonly used in computers (calculation of contact forces can be divided into several cores in parallel).

The model can undoubtedly be developed. Particularly interesting, according to the author, would be to include impurities on a part of the belt, such as oil film, into the analysis. This phenomenon is particularly dangerous because in addition to increased slip it results in greater (thus uneven) wear of the non-contaminated parts of the belt. In this case the model should be modified only slightly. It would be necessary to adopt different values of friction for each of the belt bodies.

REFERENCES

[1] Euler M.L.: Remarques sur l'effect du frottement dans l'equilibre. Mém. Acad. Sci., Berlin, 1762, pp. 265-278.

[2] Fawcett J.N.: Chain and belt drives – a review. Shock Vibrations Digest, 1981, Vol. 13, No. 5, pp. 5-12.

[3] Kruszewski J., Sawiak S., Wittbrodt E.: Metoda sztywnych elementów skończonych w dynamice konstrukcji. WNT, 1999.

[4] Kruszewski J. (ed.): Metoda sztywnych elementów skończonych. Arkady, 1975.

[5] Wojciech S.: Dynamika płaskich mechanizmów z odkształcalnymi członami, tarciem oraz luzami w parach kinematycznych (rozprawa habilitacyjna), Wydawnictwo Politechniki Gdańskiej, 1984, Z. 66.

[6] Wojciech S.: Dynamic analysis of manipulators with flexible links. Archiwum Budowy Maszyn, 1990, Vol. 37, pp. 169-188.

[7] Leamy M.J., Wasfy T.M.: Dynamic finite element modeling of belt drives. 18th Biennial Conference on Mechanical Vibration and Noise, ASME International 2001 DETC.

[8] Leamy M.J., Wasfy T.M.: Transient and Steady-State Dynamic Finite Element Modeling of Belt-Drives. ASME Journal of Dynamic Systems, Measurement, and Control, 2002, Vol. 124, No. 4, pp. 575-581.

[9] Julio G., Plante J.-S.: An experimentally-validated model of rubber-belt CVT mechanics. Mechanism and Machine Theory, 2011, 46, pp. 1037-1053.

[10] Leamy M.J., Wasfy T.M.: Analysis of belt-drive mechanics using a creep-rate-dependent friction law. Journal of Applied Mechanics, Trans. of ASME, 2002, Vol. 69, No. 6, pp. 763-771.

[11] Kim D., Leamy M.J., Ferri A.A.: Dynamic Modeling and Stability Analysis of Flat Belt Drives Using an Elastic/Perfectly Plastic Friction Law. ASME Journal of Dynamic Systems, Measurement, and Control, 2011, Vol. 133, pp. 1-10.

[12] Čepon G., Boltežar M.: Dynamics of a belt-drive system using a linear complementarity problem for the belt-pulley contact description. Journal of Sound and Vibration, 2009, Vol. 319, pp. 1019-1035.

[13] Čepon G., Manin L., Boltežar M.: Introduction of damping into the flexible multibody belt-drive model: A numerical and experimental investigation. Journal of Sound and Vibration, 2009, Vol. 324, pp. 283-296.

[14] Schindler T., Friedrich M., Ulbrich H.: Computing time reduction possibilities in multi-body dynamics, Multibody Dynamics: Computational Methods and Applications. Dordrecht, Springer, 2011, Vol. 23, pp. 239-259.

[15] Dudziak M.: Przekładnie cięgnowe. Wydawnictwo Naukowe PWN, Warszawa, 1997.

[16] Čepon G., Manin L., Boltežar M.: Experimental identification of the contact parameters between a V-ribbed belt and a pulley. Mechanism and Machine Theory, 2010, Vol. 45, pp. 1424-1433.

[17] MSC.Adams documentation.

[18] Threlfall D.C.: The Inclusion of Coulomb Friction in Mechanisms Programs with Particular Reference to DRAM. Mechanisms and Machine Theory, 1978, Vol. 13, pp. 75-483.

[19] Kragel'skij I.V., Gitis N.V.: Frikcionnye avtokolebanija. Akademija Nauk SSSR, Nauka, Moskva, 1987.

[20] Bowden F.P., Tabor D.: The friction and lubrication of solids – Part II. Oxford University Press, 1964.

[21] Dahl P.R.: A Solid Friction Model. Report No. TOR-0158(3107-18)-1, Aerospace Corporation Report, 1968.

[22] Reynolds O.: Creep theory of belt drive mechanics. The Engineer, 1847, Vol. 38.

[23] Voigt W.: Ueber innere Reibung fester Körper, insbesondere der Metalle. Annalon der Phisik, 1892, Vol. 283, pp. 671-693.

Model dyskretny płaski z tarciem suchym do analizy dynamiki przekładni pasowej

S t r e s z c z e n i e

W pracy przedstawiono pewien model przekładni pasowej służący do analizy dynamiki. Przyjęto model dyskretny płaski pasa składający się ze sztywnych członów połączonych ze sobą wzdłużnymi i skrętnymi elementami sprężysto-tłumiącymi. W modelu tym, w chwili styku członu z kołem pasowym, przyjęto model kontaktu i model tarcia suchego z uwzględnionym mikro-przemieszczeniem. Do opisu zjawisk kontaktowych wykorzystano model z odpowiednią sztywnością i tłumieniem pomiędzy stykającymi się powierzchniami, natomiast do opisu zjawiska tarcia wykorzystano uproszczony model tarcia. Ruch przekładni wywołany zostaje pod wpływem wymuszenia siłowego założonego na kołach pasowych. Równania ruchu poszczególnych członów pasa oraz kół pasowych rozwiązano numerycznie stosując metodę ze zmiennym krokiem całkowania. W dalszej części przedstawiono wyniki sił reakcji w pasie oraz sił kontaktu i tarcia pomiędzy członem a kołem pasowym w przykładowej przyjętej przekładni pasowej, uzyskane pod wpływem działania założonych na koła momentów napędowego i oporu.